

Closed-Loop Sol–Gel Transition of PEG-PEC Aqueous Solution

Bo Gyu Choi, Youn Soo Sohn, and Byeongmoon Jeong*

*Department of Chemistry, Division of Nano Sciences, Ewha Woamns University, 11-1 Daehyun-dong, Seodaemun-ku, Seoul, Korea**Received: April 16, 2007; In Final Form: June 5, 2007*

We are reporting an unusual closed-loop phase behavior of poly(ethylene glycol)- β -poly(ethyl-2-cyanoacrylate) (PEG-PEC) aqueous solutions. As the temperature increased from 0 to 60 °C, the aqueous polymer solution (12 wt %) underwent sol-to-gel and gel-to-syneresis transitions. However, the polymer aqueous solution persisted as a sol phase below 4.0 wt % as well as above 16 wt % in the same temperature range, thus forming a closed-loop gel domain in the phase diagram. The closed-loop gel domain is suggested to be a result of the balance between the aggregation and the stabilization of micelles in specific temperature and concentration ranges.

Closed-loop phase behavior has been reported in nicotine/water,¹ poly(ethylene glycol)/water,² poly(ethylene-co-butene)/poly(ethylene-co-styrene) blend,³ and poly(styrene- β -*n*-pentyl methacrylate) systems.⁴ The intermolecular forces between solutes and solvents such as dipole–dipole, dipole–induced dipole, induced dipole–induced dipole, hydrogen bond, and π – π interactions in a temperature and concentration dependent manner were suggested to explain such a closed-loop phase diagram.

Thermogelling polymers have been studied extensively as a minimally invasive depot system for drug delivery and tissue engineering.⁵ An aqueous solution of polymer with a delicate balance between hydrophobicity and hydrophilicity shows thermogelation, that is, sol-to-gel transition with increasing temperature. Hydrophobic poly(lactic acid-co-glycolic acid), polycaprolactone, polyphosphazene, poly(propylene fumarate), and chitosan coupled to hydrophilic poly(ethylene glycol) were reported as biodegradable thermogelling polymers.^{6–10}

Alkyl cyanoacrylates have been studied as biomedical materials, and some of them including butyl cyanoacrylate (Histoacryl) and octyl cyanoacrylate (Dermabond) are already on the market as tissue adhesives.¹¹ In order to design a thermogelling material based on poly(alkyl cyanoacrylate), we controlled the molecular weight of the hydrophilic poly(ethylene glycol) (PEG) and hydrophobic poly(ethyl-2-cyanoacrylate) (PEC) blocks of the poly(ethylene glycol)- β -poly(ethyl-2-cyanoacrylate) (PEG-PEC). The PEG-PEC was synthesized by addition polymerization of ethyl 2-cyanoacrylate in the presence of α -amino- ω -methoxy poly(ethylene glycol). The PEG-PEC did not show a closed-loop phase behavior when the PEG molecular weight was 550 or 1,000 Daltons. Only when the PEG molecular weight was 750, the closed-loop phase behavior was observed. The current communication will focus on the closed-loop phase behavior of PEG-PEC, and other characteristics of the PEG-PEC will be

reported in a later article. The molecular weight of the polymer was determined by ¹H NMR spectra (in CDCl₃) and gel permeation chromatography. The peaks at 1.4 ppm (CH₃CH₂ groups of PEC) and 3.6 ppm (–CH₂CH₂O– groups of PEG) in the ¹H NMR spectra were used to determine a number average molecular weight of the PEG-PEC (Supporting Information: Figure S1). When the molecular weight of PEC was larger than 500, the PEG (750)-PEC was not soluble in water. When the molecular weight of PEC was smaller than 320, the PEG (750)-PEC was freely soluble in water in a temperature range of 0–60 °C. The sol–gel transition of the PEG-PEC aqueous solution was observed when the PEC molecular weight was in a range of 350–500 daltons at a fixed PEG molecular weight of 750 daltons. In particular, closed-loop phase behavior was observed when the PEC molecular weight was in a narrow range of 400–450 daltons. The following discussion will be focused on PEG-PEC with a molecular weight of 750–400. The molecular weight and molecular weight distribution of the PEG-PEC determined by gel permeation chromatography (relative to poly(ethylene glycol) standards) were 1370 daltons and 1.2, respectively. The phase diagram of a different molecular weight PEG-PEC (750–450; $M_n \sim 1450$ daltons; $M_w/M_n \sim 1.2$) is compared in Supporting Information (Figure S2). Briefly, as the PEC molecular weight of the PEG-PEC increased from 400 to 450 daltons at a fixed PEG molecular weight of 750 daltons, the sol-to-gel transition temperature and the critical gel concentration decreased, whereas the gel window and maximum gel modulus increased.

The phase transition of PEG-PEC aqueous solution was studied by the test tube inverting method and dynamic mechanical analysis.^{12,13} PEG-PEC aqueous solutions underwent a sol-to-gel transition as the temperature increased in a concentration range of 4.0–14 wt % (Figure 1a). Instead of forming a three-dimensional network as a whole, the transparent solutions underwent a sol-to-syneresis transition, a macroscopic phase separation between polymers and water, at lower concentrations than 4.0 wt %, as the temperature increased. Interestingly, the

* To whom correspondence should be addressed. Fax: 82-2-3277-3419. E-mail: bjeong@ewha.ac.kr.

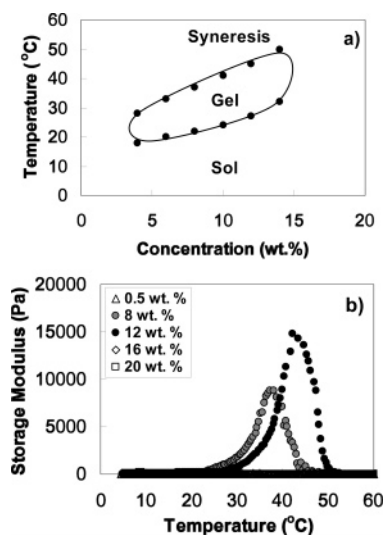


Figure 1. (a) Phase diagram of PEG-PEC aqueous solutions determined by the test tube inverting method. Each data point is an average of three measurements. (b) Dynamic mechanical analysis of the PEG-PEC aqueous solutions as a function of the temperature and concentration. The data were collected under a controlled stress (4.0 dyn/cm^2) and a frequency of 1.0 rad/s . The heating rate was $0.3 \text{ }^\circ\text{C/min}$. The legends are the concentrations of the polymer in water.

sol-to-gel transition temperature of the PEG-PEC aqueous solution increased as the concentration increased. This behavior is opposite to the previous thermogelling polymer aqueous solutions such as poly(lactic acid-co-glycolic acid), polycaprolactone, polyphosphazene, poly(propylene fumarate), and chitosan, where the sol-to-gel transition temperature decreased as the polymer concentration increased.^{6–10} In addition, the polymer aqueous solution at 16 wt % or above kept its sol phase in a temperature range of $0\sim 60 \text{ }^\circ\text{C}$, thus forming a closed-loop gel domain in the phase diagram.

Dynamic mechanical analysis also confirmed the closed-loop phase diagram of the PEG-PEC aqueous solution. As the temperature increased, a sol-to-gel transition accompanying an abrupt increase in storage modulus was observed only for 8.0 and 12 wt % polymer aqueous solutions (Figure 1b). However, a significant increase in modulus was not observed at a low concentration of 0.5 wt % as well as at high concentrations of 16 and 20 wt %. As the temperature increased, the storage modulus of 12 wt % of the PEG-PEC aqueous solution increased to about $15\,000 \text{ Pa}$ at $42 \text{ }^\circ\text{C}$ and decreased because of the gel-to-syneresis transition. The maximal storage modulus of an 8.0 wt % PEG-PEC aqueous solution observed at $37 \text{ }^\circ\text{C}$ was 1.7 times lower than that of the 12 wt % polymer aqueous solution.

Figure 2 shows photos of the PEG-PEC aqueous solutions taken at 5 and $30 \text{ }^\circ\text{C}$. At $5 \text{ }^\circ\text{C}$, all of the polymer solutions of 0.5, 12, and 20 wt % are in a transparent sol state. As the temperature increased to $30 \text{ }^\circ\text{C}$, the 0.5 wt % aqueous solution underwent syneresis, whereas the 12 wt % aqueous solution turned into a gel. However, the 20 wt % aqueous solution remained in a sol state at $30 \text{ }^\circ\text{C}$.

To understand the mechanism of the closed-loop phase behavior, fluorescence spectroscopy and dynamic/static light scattering of the PEG-PEC aqueous solution were studied. The PEG-PECs consisting of hydrophilic PEG and hydrophobic PEC form micelles in water. Micelle formation was confirmed by the partitioning of a hydrophobic dye (2-anilinonaphthalene) into a micelle core.¹⁴ The emission wavelength of 2-anilinon-

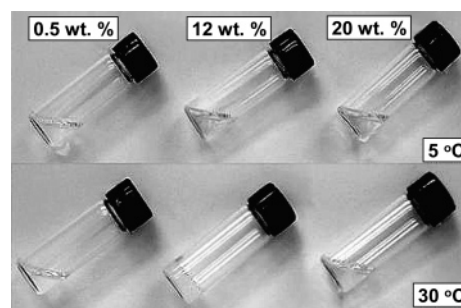


Figure 2. Photos of the PEG-PEC aqueous solutions at 5 and $30 \text{ }^\circ\text{C}$ and at 0.5, 12, and 20 wt %. Only the 12 wt % aqueous solution at $30 \text{ }^\circ\text{C}$ showed a gel formation.

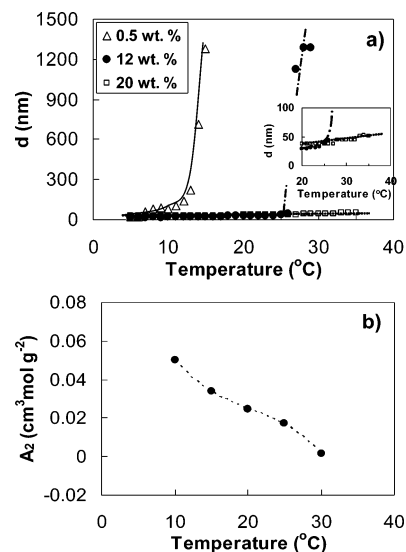


Figure 3. (a) Apparent micelle sizes determined by dynamic light scattering as a function of temperature. The legends are concentrations of the polymer in water. (b) Second virial coefficient of the PEG-PEC in water determined by static light scattering as a function of temperature.

aphthalene in the fluorescence spectra sensitively decreased from 435 to 395 nm as the polarity of the medium decreased. The critical micelle concentration (CMC) of PEG-PEC determined by extrapolating the shift in emission wavelength as a function of polymer concentration was $1.6 \times 10^{-3} \text{ wt } \%$ at room temperature ($\sim 20 \text{ }^\circ\text{C}$). The micelle size of PEG-PEC determined by dynamic light scattering is shown as a function of temperature and concentration (Figure 3a and Supporting Information Figure S3). In a low concentration (0.5 wt %), the apparent size increased from 20 nm ($5 \text{ }^\circ\text{C}$) to 1200 nm ($15 \text{ }^\circ\text{C}$), indicating a sol-to-syneresis transition at $15 \text{ }^\circ\text{C}$. The polymer concentration was not high enough to form a gel as a whole; thus, syneresis occurred. The micelle size in the 12 wt % of PEG-PEC aqueous solution suddenly increased from 20 nm ($5 \text{ }^\circ\text{C}$) to 1300 nm at $27 \text{ }^\circ\text{C}$ at which the aqueous solution underwent sol-to-gel transition. This finding suggests that micellar aggregation is the mechanism of the sol-to-gel transition of the PEG-PEC aqueous solution. However, the micelle size in the 20 wt % PEG-PEC aqueous solution kept constant at about 50 nm in a temperature range of $5\sim 35 \text{ }^\circ\text{C}$, suggesting the stability in a sol state in this composition of the polymer and water mixture.

Static light scattering gave information on the second virial coefficient (A_2) of the polymer as a function of temperature. A_2 is a measure of solubility of the polymer in a solvent. A large second virial coefficient indicates favorable interactions between

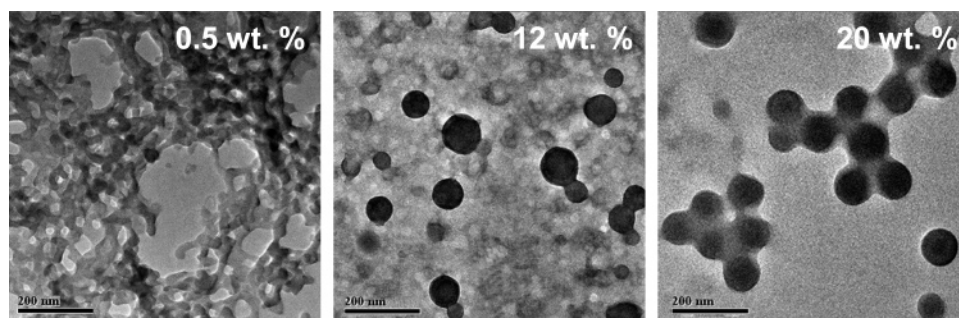


Figure 4. Transmission electron microscopic images of the PEG-PEC aqueous solutions at 20 °C prepared at 0.5, 12, and 20 wt %. The scale bar is 200 nm.

the solvent and polymers.^{15,16} When we assume that the PEG-PEC micelles are in a spherical shape, A_2 can be obtained by the Debye plot.^{17,18}

$$KC/R_{vv} = 1/M_w + 2A_2C$$

$K = 4\pi^2 n^2 (dn/dc)^2 / N_A \lambda^4$, C is the concentration of a PEG-PEC aqueous solution, and R_{vv} is the excess Rayleigh ratio. The concentration C was varied over 0.001–0.01 wt %. Variables M_w and A_2 can be calculated from the y intercept and the slope in the Debye plot, respectively. The molecular weight of a micelle, M_w , is equal to the molecular weight of the PEG-PEC (1150 daltons) times the aggregation number of a micelle. The second virial coefficients (A_2) were plotted against temperature (Figure 3b). The second virial coefficient decreased from 0.05 to 0.001 ($\text{cm}^3 \text{mol g}^{-2}$) as the temperature increased from 10 to 30 °C, suggesting that water changed from a good solvent to a poor solvent for PEG-PEC as the temperature increased in low polymer concentrations. The decreased solubility of the PEG-PEC in water drove the aggregation of the micelles, resulting in syneresis at low concentrations (<4.0 wt %) or a sol-to-gel transition at medium concentrations of 4.0–14 wt %.

The polymer morphology in water was investigated using a high resolution- transmission electron microscope (TEM). In the 0.5 wt % PEG-PEC aqueous solution, polymers were extensively aggregated and lost their micellar shape at 20 °C because they were in a syneresis state. A TEM image focused on polymer aggregates was chosen at this concentration. The TEM images developed at 12 and 20 wt % PEG-PEC aqueous solutions showed spherical micelles at 20 °C (Figure 4). These data were consistent with the results of dynamic light scattering, where micelles exist in a stable form at 20 wt %, whereas they are aggregated at 0.5 wt % at 20 °C.

Any spontaneous process involves a decrease in free energy ($\Delta G = \Delta H - T\Delta S < 0$); thus, an endothermic spontaneous process ($\Delta H > 0$) should be compensated by an entropic increase ($\Delta S > 0$). As the temperature increased at a fixed polymer concentration (12 wt %), the solution underwent sol-to-gel and gel-to-syneresis transitions that involved aggregation of the micelles and dehydration. Those transitions are endothermic processes as shown in the thermogram (Figure 5), suggesting the entropically driven process. As the concentration increases at a fixed temperature such as 30 °C, the micelle concentration of the system increases, and an entropy gain through the aggregation of the micelles decreases, and thus favors the system soluble sol at a high polymer concentration of 20 wt % at 30 °C and forms a closed-loop phase diagram.

To conclude, PEG-PEC aqueous solutions showed a closed-loop gel domain at a specific concentration and temperature range. As the temperature increased, solubility of the PEG-PEC

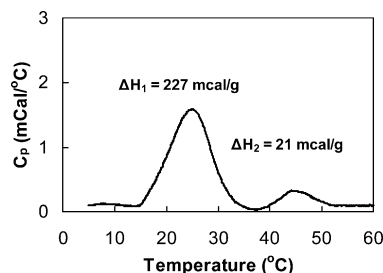


Figure 5. Thermogram of PEG-PEC aqueous solution (12 wt %). Heating rate was 1.0 °C/min. The two endothermic peaks at ΔH_1 centered at 25 °C and at ΔH_2 centered at 45 °C are correlated to the sol-to-gel and gel-to-syneresis transitions, respectively.

decreased as suggested by a decrease in the second virial coefficient. Such a change drives the micelles to aggregate to syneresis in low polymer concentrations (<4.0 wt %) and to gelation in a polymer concentration range of 4.0–12 wt %. On the other hand, the micelles were quite stable when the polymer concentration was higher than 16.0 wt %, and the polymer aqueous solution existed in a stable sol state, resulting in a closed-loop gel domain in the phase diagram. The closed-loop gel domain is suggested to be a result of the balance between the aggregation and the stabilization of micelles in specific temperature and concentration ranges.

Acknowledgment. This work was supported by the SRC program of MOST/KOSEF through the Center for Intelligent NanoBio Materials at Ewha Womans University (Grant R11-2005-008-0000-0) and the Korea Research Foundation grant funded by the Korean Government (MOEHRD, Grant KRF-2005-C00300 and KRF-2004-005-C00090). B.G.C. was supported by the Seoul Science Fellowship.

Supporting Information Available: Experimental protocols for synthesis; characterization methods of the PEG-PEC; ^1H NMR spectra of the PEG-PEC; effects of the PEC molecular weight of the PEG-PEC on the phase diagram; storage modulus and dynamic light scattering data of the PEG-PEC aqueous solutions as a function of temperature. This material is available free of charge via the Internet at <http://www.pubs.acs.org>.

References and Notes

- (1) (a) Hudson, C. S. Z. *Phys. Chem. (Munich)* **1904**, 47, 113–115. (b) Ruzette, A.-V. *Nat. Mater.* **2002**, 1, 85–87.
- (2) Dormidontova, E. E. *Macromolecules* **2002**, 35, 987–1001.
- (3) Chong, H.; Hu, C.; He, A.; Zhang, C.; Fan, G.; Dong, J.-Y.; Han, C. C. *Macromol. Rapid Commun.* **2005**, 26, 973–978.
- (4) (a) Ryu, D. Y.; Jeong, U.; Kim, J. K.; Russel, T. P. *Nat. Mater.* **2002**, 1, 114–117. (b) Lee, D. H.; Kim, H. J.; Kim, J. K. *Macromol. Symp.* **2006**, 240, 123–129.

- (5) Jeong, B.; Kim, S. W.; Bae, Y. H. *Adv. Drug Delivery Rev.* **2002**, *54*, 37–51.
- (6) (a) Jeong, B.; Bae, Y. H.; Kim, S. W. *Macromolecules* **1999**, *32*, 7064–7069. (b) Yu, L.; Zhang, H.; Ding, J. *Angew. Chem., Int. Ed.* **2006**, *45*, 2232–2235.
- (7) Bae, S. J.; Joo, M. K.; Jeong, Y.; Kim, S. W.; Lee, W. K.; Sohn, Y. S.; Jeong, B. *Macromolecules* **2006**, *39*, 4873–4879.
- (8) Lee, B. H.; Lee, Y. M.; Sohn, Y. S.; Song, S. C. *Macromolecules* **2002**, *35*, 3876–3879.
- (9) Behraves, E.; Shung, A. K.; Jo, S.; Mikos, A. *Biomacromolecules* **2002**, *3*, 153–158.
- (10) Chenite, A.; Chaput, C.; Wang, D.; Combes, C.; Buschmann, M. D.; Hoemann, C. D.; Leroux, J. C.; Atkinson, B. L.; Binette, F.; Selmani, A. *Biomaterials* **2000**, *21*, 2155–2161.
- (11) Couvreur, P.; Couarraze, G.; Devissaguet, J.; Puisieux, F. Nanoparticles: preparation and characterization. In *Microencapsulation: Methods and Industrial Applications*; Benita, S., Ed.; Marcel Dekker, New York, 1996; pp 183–211.
- (12) Shim, W. S.; Yoo, J. S.; Bae, Y. H.; Lee, D. S. *Biomacromolecules* **2005**, *6*, 2930–2934.
- (13) Wilder, E. A.; Hall, C. K.; Khan, S. A.; Spontak, R. J. *Langmuir* **2003**, *19*, 6004–6013.
- (14) Arotcarena, M.; Heise, B.; Ishaya, S.; Laschewsky, A. *J. Am. Chem. Soc.* **2002**, *124*, 3787–3793.
- (15) Villetti, M. A.; Borsali, R.; Crespo, J. S.; Soldi, V.; Fukada, K. *Macromol. Chem. Phys.* **2004**, *205*, 907–917.
- (16) Quintana, J. R.; Janez, M. D.; Villacampa, M.; Katime, I. *Macromolecules* **1995**, *28*, 4139–4143.
- (17) Bilalis, P.; Zorba, G.; Pitsikalis, M.; Hadjichristidis, N. *J. Polym. Sci., Part A: Polym. Chem.* **2006**, *44*, 5719–5728.
- (18) Mya, K. Y.; Li, X.; Chen, L.; Ni, X.; Li, J.; He, C. *J. Phys. Chem. B* **2005**, *109*, 9455–9462.